Received: 27 May 2019 | Revised: 6 August 2019 | Accepted: 7 August 2019

DOI: 10.1111/1755-0998.13089

RESOURCE ARTICLE

MOLECULAR ECOLOGY RESOURCES WILEY

Multiscale resistant kernel surfaces derived from inferred gene flow: An application with vernal pool breeding salamanders

Kristopher J. Winiarski[1,2] | William E. Peterman[3] | Andrew R. Whiteley[4] | Kevin McGarigal[1]

[1]Department of Environmental Conservation, University of Massachusetts, Amherst, MA, USA

[2]Northeast Climate Adaptation Science Center, University of Massachusetts, Amherst, MA, USA

[3]School of Environment and Natural Resources, Ohio State University, Columbus, OH, USA

[4]W.A. Franke College of Forestry and Conservation, Wildlife Biology Program, University of Montana, Missoula, MT, USA

Correspondence
Kristopher J. Winiarski, Department of Environmental Conservation, University of Massachusetts, Amherst, MA, USA.
Email: withakri@gmail.com

Abstract

The importance of assessing spatial data at multiple scales when modelling species–environment relationships has been highlighted by several empirical studies. However, no landscape genetics studies have optimized landscape resistance surfaces by evaluating relevant spatial predictors at multiple spatial scales. Here, we model multiscale/layer landscape resistance surfaces to estimate resistance to inferred gene flow for two vernal pool breeding salamander species, spotted (*Ambystoma maculatum*) and marbled (*A. opacum*) salamanders. Multiscale resistance surface models outperformed spatial layers modelled at their original spatial scale. A resistance surface with forest land cover at a 500-m Gaussian kernel bandwidth and normalized vegetation index at a 100-m Gaussian kernel bandwidth was the top optimized resistance surface for *A. maculatum*, while a resistance surface with traffic rate and topographic curvature, both at a 500-m Gaussian kernel bandwidth, was the top optimized resistance surface for *A. opacum*. Species-specific resistant kernels were fit at all vernal pools in our study area with the optimized multiscale/layer resistance surface controlling kernel spread. Vernal pools were then evaluated and scored based on surrounding upland habitat (local score) and connectivity with other vernal pools on the landscape, with resistant kernels driving vernal pool connectivity scores. As expected, vernal pools that scored highest were in areas within forested habitats and with high vernal pool densities and low species-specific landscape resistance. Our findings highlight the success of using a novel analytical approach in a multiscale framework with applications beyond vernal pool amphibian conservation.

KEYWORDS

Ambystoma maculatum, *Ambystoma opacum*, circuit theory, isolation by resistance, landscape genetics, resistance surface, ResistanceGA

1 | INTRODUCTION

In ecological contexts, scale refers to the spatial and temporal interactions of organisms with their environment (McGarigal, Wan, Zeller, Timm, & Cushman, 2016). Foundational ecological theory on the importance of incorporating spatial scale in ecological research (Addicot et al., 1987; Levin, 1992; Wiens, 1989) has recently been validated by several empirical studies evaluating environmental and anthropogenic predictors in a multiscale context, which involves consideration of landscape variables not just at their original scale but at multiple spatial and/or temporal scales (McGarigal et al., 2016). This includes studies evaluating predictors at multiple scales

with (i) species–habitat relationships (Peterman, 2018) (Chambers, Cushman, Medina-Fitoria, Martínez-Fonseca, & Chávez-Velásquez, 2016; Grand, Buonaccorsi, Cushman, Griffin, & Neel, 2004; Johnson, Parker, Heard, & Gillingham, 2002; Timm, McGarigal, Cushman, & Ganey, 2016), (ii) species abundance (Chandler & Hepinstall-Cymerman, 2016) and iii) landscape resistance (Cushman, Elliot, Macdonald, & Loveridge, 2016; Krishnamurthy et al., 2016; Zeller et al., 2014; Zeller, Vickers, Ernest, & Boyce, 2017). Evaluating environmental and anthropogenic predictors measured at multiple scales provides a more nuanced understanding of how species relate to and utilize their environment, suggesting the applicability of such an approach to a broad range of ecological analyses and disciplines (McGarigal et al., 2016).

The goal of landscape genetics is to understand gene flow and spatial genetic patterns within species in response to landscape composition and configuration with a reliance on conceptual ideas and tools from landscape ecology, population genetics and spatial statistics (Manel & Holderegger, 2013; Manel, Schwartz, Luikart, & Taberlet, 2003). Understanding genetic connectivity and the spatial layers driving (or limiting) gene flow and the resulting spatial genetic patterns is crucial if applied conservation goals include the management of the landscape to restore genetic connectivity to isolated populations to ensure long-term viability (Greenwald, 2010; Whiteley, Fitzpatrick, Funk, & Tallmon, 2015), or the management of the landscape to allow for species movement or rapid adaptation to future landscape and environmental changes such as those driven by climate change (Velo-Antón, Parra, Parra-Olea, & Zamudio, 2013).

Landscape genetics studies have previously been conducted at multiple spatial 'levels' (similar to the hierarchical levels of habitat selection as defined by Johnson, 1980) to compare differences in landscape predictors of gene flow both within sampling sites and between sampling sites, between individuals or between management areas, but only recently has a landscape genetics study estimated landscape resistance (LR) with environment and anthropogenic predictors at multiple scales within a single spatial level (Zeller et al., 2017). Advances have also been made with analytical approaches to measure landscape resistance (reviewed by Richardson, Brady, Wang, & Spear, 2016), including the true optimization of landscape resistance surfaces (LRSs) (Hanks & Hooten, 2013; Peterman, 2018) vs. a pseudo-optimization of LRSs (Shirk, Wallin, Cushman, Rice, & Warheit, 2010), which has been found to have higher type I error rates than analytical approaches using a true optimization approach (Peterman et al., 2019). LRS optimization is one such ecological analysis where models could be improved by incorporating anthropogenic and environmental drivers of gene flow at multiple spatial scales.

Here, we optimized multiscale/layer LRS for two ambystomatid salamanders. We used genetic distance data sets of spotted salamanders (*Ambystoma maculatum*; AMMA) and marbled salamanders (*A. opacum*; AMOP) from a recent study by Whiteley, McGarigal, and Schwartz (2014), which found that although ecologically very similar, AMMA and AMOP had differing genetic structures and rates of inferred gene flow across the landscape. We hypothesized that for both species, inferred gene flow would be highest through natural areas that facilitate movement and survival in our study area, such as forested habitats with high densities of vernal pools (VPs) with topography well suited for the physiological conditions required for salamander migration and dispersal (e.g. specific range of topographic wetness), and that inferred gene flow would be more constrained in areas with high densities of roads and urban development, or by natural topographic features on the landscape such as ridges or large rivers (see Table 1 for supporting literature justifying modelled spatial layers). We predicted that the differences found in the genetic patterns and inferred gene flow between AMMA and AMOP would potentially be explained by species-specific differences in the relationships between environmental, topographic and anthropogenic features with LR and differences in the species-specific optimized spatial scales. We also sought to identify which VPs across our study area were most important for species-specific gene flow based on their landscape context and inferred connectivity at local, neighbourhood and regional spatial levels.

2 | MATERIALS AND METHODS

2.1 | Study site

Our study was conducted in the Pioneer Valley of western Massachusetts (Figure 1). The Pioneer Valley is bisected by the Connecticut River and is characterized in the north by an agricultural valley interspersed with residential development and in the southcentral by high-density urban development. The Pioneer Valley also contains high elevation features (e.g. Holyoke Range) and transitions gradually to the west and east into areas of higher elevation dominated by forest interspersed with lower density residential development.

2.2 | Study species

2.2.1 | *Ambystoma maculatum* (AMMA)

Individuals migrate from the surrounding upland to VPs in the spring to breed (Petranka, 1998). AMMA dispersal distances have not been directly quantified, but migration distances have been recorded up to 467m from the emigrated VP (McDonough & Paton, 2007; Veysey, Babbitt, & Cooper, 2009). Using genetic data, dispersal distance for AMMA was estimated to be 2,050 m (Peterman et al., 2015). AMMA are ca. 15–25 cm in length with a generation time of ca. 7–8 years (Petranka, 1998). In our study area, AMMA are relatively abundant with high effective population sizes (Whiteley et al., 2014).

2.2.2 | Ambystoma opacum (AMOP)

Individuals migrate from the surrounding upland to VPs in the fall to breed when VPs are dry (Petranka, 1998). Natal philopatry is relatively high with 96.4% of experienced breeders and 91% of first-time breeders, returning to their natal VP to breed (Gamble, McGarigal,

TABLE 1 Spatial layers used to model landscape resistance of spotted (*Ambystoma maculatum*) and marbled (*A. opacum*) salamanders and our justification for their inclusion in landscape resistance modelling process, derivation and supporting literature where a particular spatial layer was found to be an important driver of gene flow in a previous study

Spatial Layers	Original spatial resolution (m)	Justification	Source	Derivation	Supporting literature
Topographic curvature	5	High values limit dispersal ability and gene flow	DEM Massachusetts GIS (http://www.mass.gov/anf/research-and-tech/it-serv-and-support/application-serv/office-of-geographic-information-massgis/datalayers/)	Total curvature (see Jenness, 2013)	Funk et al., (2005); Murphy et al., (2010)
Impervious surfaces	30	Impedes movement and causes direct mortality	Massachusetts Conservation Assessment and Prioritization System (http://www.umasscaps.org/data_maps/data.html)	Percent impervious	Murphy et al., (2010)
Forest land cover (1971, 1985, 1999, 2005)	30	Enables movement and gene flow	Massachusetts GIS (http://www.mass.gov/anf/research-and-tech/it-serv-and-support/application-serv/office-of-geographic-information-massgis/datalayers/)	Binary forest land cover layer	Greenwald, Purrenhage, et al. (2009); Goldberg and Waits (2010)
Normalized difference vegetation index	30	High values enable movement and gene flow	Global Web Enabled Landsat Data website (http://globalweld.cr.usgs.gov/)	Normalized difference vegetation index (NDVI) value generated from Band3_TOA_REF and Band4_TOA_REF	Spear and Storfer, (2008)
Potential vernal pools	NA	High densities of pools enable movement and gene flow	Massachusetts GIS; Natural Heritage and Endangered Species Program (http://www.mass.gov/anf/research-and-tech/it-serv-and-support/application-serv/office-of-geographic-information-massgis/datalayers/)	Photograph interpretation of colour infrared aerial photographs by the Massachusetts Natural Heritage and Endangered Species Program (Burne 2001)	
Topographic position index	5	Different features may enable or impede movement and gene flow	DEM Massachusetts GIS (http://www.mass.gov/anf/research-and-tech/it-serv-and-support/application-serv/office-of-geographic-information-massgis/datalayers/)		Funk et al., (2005); Murphy et al., (2010)
Traffic rate	30	Higher values impede movement and gene flow	Mass Conservation Assessment and Prioritization System (http://www.umasscaps.org/data_maps/data.html)	Intensity of road traffic. Probability of an animal crossing being hit given traffic rate	Richardson, (2012); Coster et al., (2015)
Topographic wetness index	30	Movement and gene flow impeded by areas too 'wet' or too 'dry'	Designing Sustainable Landscapes (http://www.umass.edu/landeco/research/dsl/products/dsl_products.html)		Richardson, (2012)
Water flow rate	30	High flow rates impede movement and gene flow	Massachusetts Conservation Assessment and Prioritization System (http://www.umasscaps.org/data_maps/data.html)	Log-scaled FP8 Flow accumulation from DEM	Coster et al., (2015)

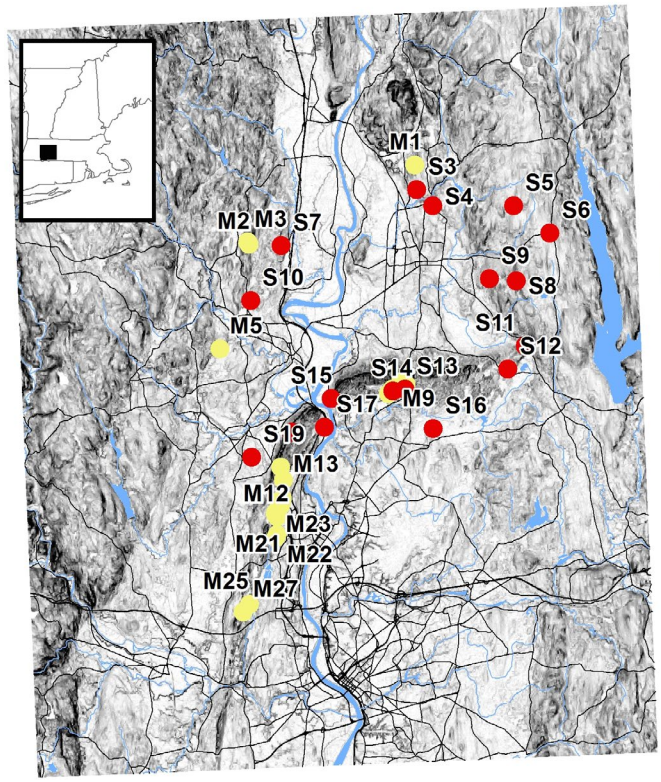

FIGURE 1 Study area in the Pioneer Valley in western Massachusetts. Nineteen vernal pools were sampled for larval spotted salamanders (Ambystoma maculatum) (S1–S19), and twenty-nine vernal pools were sampled for larval marbled salamanders (A. opacum) (M1-M29). Larval A. maculatum were collected during the summer of 2007 and 2008, and larval A. opacum were collected during the spring of 2010. Whiteley et al., 2014 found model support for no population-level clustering for A. maculatum (K = 1) but did find evidence for population-level clustering for A. opacum (K = 3; M1-M3 and M6-10, M11-24 and M29, and M5 and M25-M27)

& Compton, 2007). Dispersal distances have been recorded up to 1,300 m for juvenile dispersers and 440 m for adult dispersers (Gamble et al., 2007). AMOP are c. 9–11 cm in length with generation time of ca. 5–6 years (Petranka, 1998). In our study area, AMOP are at the northern extent of their range and at low population sizes with low effective population sizes (Whiteley et al., 2014). AMOP are state-threatened in Massachusetts (M.F.L c.131A and regulations 321 CMR 10.00).

2.3 | Population sampling

We collected larval AMMA and AMOP from 19 VPs (S1–S19) and 29 VPs (M1-M29), respectively, distributed across the Pioneer Valley (Figure 1). VPs varied in size but were all smaller than one hectare. Larval AMMA were collected during the summer of 2007 and 2008, and larval AMOP were collected during the spring of 2010. We sampled VPs by visually scanning the VP perimeter after dusk with a headlamp. The specific number of individual larvae sampled varied by VP (AMMA mean = 25.25, range = 12–50 larvae; AMOP mean = 29, range = 11–30 larvae) and depended on local population size and reproductive success prior to sampling (Table 2; Whiteley et al., 2014). A tissue sample (tip of tail) was taken from each individual as a source of genetic material, and individuals were then released back into the VP (see Whiteley et al. (2014) for more detail regarding larval salamander sampling).

2.4 | Landscape genetics analysis

We extracted DNA from each larval tail clip with a standard salt precipitation procedure. AMMA and AMOP were genotyped at eight microsatellite loci: *AmaD321*, *AmaD95*, *AmaD287*, *AmaD328*, *AmaC40*, *AjeD23*, *AmaD49*, *AmaD184* and *AMaD49*, *Aop36*, *AmaD95*, *AmaD184*, *AmaD42*, *AmaD328*, *AjeD23*, *AmaD321*, respectively (Julian et al., 2003a,b; Croshaw et al., 2005). We used Qiagen multiplex buffer (Qiagen, Inc.) with the manufacturer's recommending thermal cycler profile for microsatellite amplification. We used an Applied Biosystems 3130×1 capillary sequencer to determine the size of PCR fragments. We used Gene Mapper and PeakScanner (Applied Biosystems) to score individual genotypes based on the ROX 500 size standard run with each individual. Whiteley et al. (2014) reported detailed population genetic analyses for this same set of populations for both species, including an analysis of the influence of full-sibling families on population genetic structure. The practice of removing full-siblings for some population genetic analyses has recently been called into question (Waples & Anderson, 2017), but amphibian-focused studies have recommended removing siblings to avoid biased inference (Goldberg & Waits, 2010; Peterman, Brocato, Semlitsch, & Eggert, 2016). Based on the previous analysis of our focal populations, inclusion of full-sibling families in the analysis increased the signal of genetic differentiation (Whiteley et al., 2014). Therefore, we chose to limit the final data set to a single randomly sampled full-sibling per family from each VP for each species.

We calculated chord distance (D_C) between local populations with GENODIVE version 2.0 (Meirmans & Tienderen, 2004). We used D_C as our metric of genetic distance instead of F_{ST} as it has been found to better differentiate genetically similar populations, provides less biased estimates of differentiation and relies on fewer assumptions (Libiger, Nievergelt, & Schork, 2009; Peterman, Connette, Semlitsch, & Eggert, 2014). We discarded two AMMA local populations (S1 and S2) that contained 10 or fewer estimated unique full-sibling families

TABLE 2 Number of spotted salamanders (*Ambystoma maculatum*) and marbled salamanders (*A. opacum*) individuals genotyped (*N*) and the number of estimated full-sibling families (Families) for vernal pools sampled in Massachusetts, USA

A. maculatum			A. opacum		
Site name	*N*	Families	Site name	*N*	Families
S1	27	18	M1	30	10
S2	30	24	M2	30	18
S3	20	12	M3	30	15
S4	12	10	M4	30	2
S5	30	16	M5	29	17
S6	30	13	M6	31	10
S7	30	16	M7	30	17
S8	30	18	M8	30	23
S9	19	14	M9	30	15
S10	30	19	M10	30	18
S11	20	14	M11	11	3
S12	20	14	M12	30	12
S13	50	36	M13	29	14
S14	32	26	M14	30	2
S15	20	17	M15	30	21
S16	20	13	M16	30	10
S17	20	15	M17	30	21
S18	20	15	M18	29	13
S19	20	13	M19	29	13
			M20	30	12
			M21	30	19
			M22	30	17
			M23	30	22
			M24	30	7
			M25	30	11
			M26	30	8
			M27	20	13
			M28	30	1
			M29	30	8

and seven AMOP local populations (M4, M11, M14, M24, M26, M28 and M29) that contained 10 or fewer estimated full-sibling families due to the lower overall population sizes prior to the calculation of genetic distance. We fit an isolation-by-distance model for AMMA and AMOP with pairwise D_C as the response variable and Euclidean distance (m) as the independent variable using a linear mixed-effects model (R package lme4; Bates, Mächler, Bolker, & Walker, 2015) with a maximum-likelihood population effects (MLPE) parameterization to account for the nonindependence of values within pairwise distance matrices (Clarke, Rothery, & Raybould, 2002).

2.5 | Multiscale evaluation of spatial layers

We evaluated 13 environmental and anthropogenic spatial layers that we hypothesized could predict the gene flow and genetic patterns of AMMA and AMOP across the study area (Table 1). Spatial layers included the following: 1) topographic curvature, which we calculated using DEM Surface Tools (Jenness, 2013); 2) impervious surfaces (2005); 3–6) forest land cover at 4 temporal snapshots (1971, 1985, 1999 and 2005); 7) normalized difference vegetation index from July 2012 (NDVI); 8) potential VPs (2,081 unique VPs in our study area); 9) slope; 10) topographic position index (TPI); 11) traffic rate; 12) topographic wetness index (TWI); and 13) water flow rate (Figure 2). We increased the cell resolution for all spatial layers from the original resolution to 60m using the Resample tool in ArcGIS to make our analysis computationally feasible (Pearson's correlations for our spatial layers at their original 60m pixel size are shown in Supporting Informatioon 1). No correlation exceeded |0.70|. To evaluate surfaces at multiple spatial scales, we smoothed all resulting 60-m surfaces with the R package gridkernel (https://github.com/ethan-plunkett/gridkernel) using a Gaussian kernel with 100-m, 500-m, 1,000-m, 1,500-m and 2,000-m bandwidths to control the spread of the Gaussian kernel. A Gaussian kernel gives greater weight to pixels closer to the focal pixel, which incorporates spatial scale more realistically than alternative approaches such as moving window analyses. The bandwidth sizes used to smooth our spatial layers captured a range that was relevant to the ecology of our study species based on the spatial extent of our study area, inferred scale of salamander habitat selection and known dispersal distances.

2.6 | Multiscale single-layer LRS optimization

We used the R package 'ResistanceGA' (Peterman, 2018; https://github.com/wpeterman/ResistanceGA) to first optimize a LRS for each spatial layer independently to (i) determine the best supported Gaussian kernel bandwidth for each spatial layer and then (ii) to fit multiscale/layer LRSs based on those best supported univariate layers. ResistanceGA uses a genetic algorithm (R package GA; Scrucca, 2013) and the concepts of evolution and natural selection to optimize the functional transformation, shape and maximum resistance values of a LRS. During optimization, each spatial layer was transformed into a LRS using 1 of 8 different functional transformations (e.g. monomolecular or Ricker family transformations). We limited the functional transformation in our analysis to monomolecular transformation for all spatial layers as we felt that the Ricker function may overfit to the data and was biologically unreasonable for all of our spatial layers except for TWI. We felt the Ricker was biologically reasonable for TWI as we hypothesized that resistance could be high at low TWI values, low at mid-TWI values and high at high TWI values. For each iteration, ResistanceGA fits a linear mixed-effects model to the data (R package lme4; Bates et al., 2015). Pairwise genetic distance (here chord distance, D_C) between sampled populations was the dependent variable, and scaled and centred effective pairwise resistance distance between the populations was the independent variable. This mixed-effects model uses a maximum-likelihood population effects parameterization with population as a random effect to account for the nonindependence of values within pairwise distance matrices (Clarke et al., 2002).

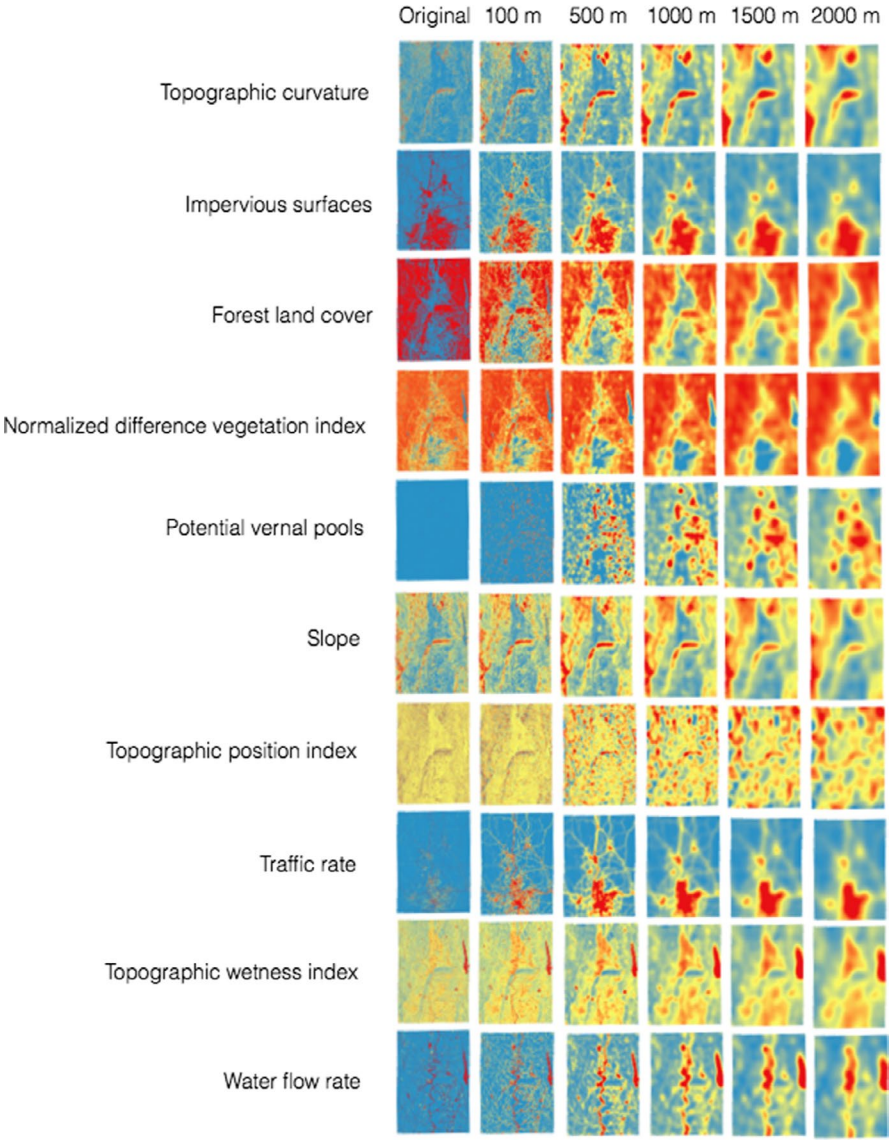

FIGURE 2 Spatial surfaces used to model landscape resistance for spotted (Ambystoma maculatum) and marbled (A. opacum) salamanders including topographic curvature, impervious surfaces (2005), forest land cover (1999), normalized difference vegetation index (July 2010), potential vernal pools, slope, topographic position index, traffic rate, topographic wetness index and water flow rate. Forest land cover at 1971, 1985 and 2005 was also included in the analysis (not shown here). Each spatial surface was evaluated at its original resolution (60 m) and at multiple spatial scales with surfaces smoothed using a Gaussian kernel at 100-m, 500-m, 1,000-m, 1,500-m and 2,000-m bandwidths. Colours of surfaces represent low (blue), mid (yellow) and high (red) values

Resistance distances were calculated between VP populations using CIRCUITSCAPE (version 4.0.3; McRae, Dickson, Keitt, & Shah, 2008) with an eight-neighbour connection scheme. AICc (Akaike's information criterion corrected for small/finite sample size; Akaike, 1998) was the objective criterion the genetic algorithm worked to minimize during the iterative optimization process. R code to implement our univariate multiscale optimization procedure using ResistanceGA is provided online (https://github.com/withakri/Resistance-surface-optimization).

2.7 | Multiscale/layer LRS optimization

We optimized multiscale/layer LRSs as follows. First, we restricted consideration to the best supported (delta AICc <5) single layers at their best spatial scale. We then computed Pearson's correlation coefficients for each pairwise combination of the retained univariate layers at their best spatial scale. Next, we fit pairwise combinations of the retained covariates at their best spatial scale but restricted from consideration any combinations of covariates with correlations >0.7 to avoid multicollinearity (Supporting Information S2 and S3). We limited multilayer models to a maximum of two spatial layers due to the long computational times needed to optimize more complex models. We found that the multiscale/layer LRSs that we derived from this restricted set of single-layer spatial scales did not outperform the best supported single-layer LRSs, based on AICc. We suspected that this might be due to the increased correlations between spatial layers at their optimized spatial scale (Supporting Information S2 and S3), despite the restrictions we imposed to safeguard against multicollinearity. In addition, we suspected that this approach might be masking scale complementarity among spatial layers; for example a fine-scale spatial layer complementing a coarse-scale spatial layer. Consequently, we then selected our top two performing single-layer LRSs for AMOP and AMMA and fit all two-layer combinations of these two covariates at all spatial scales, including the original scale (60 m) and smoothed spatial layers at all bandwidths (100 m, 500 m, 1,000 m, 1,500 m and 2,000 m). Again, we restricted from consideration any pairwise combinations of the two covariates (at any scale) with correlations >0.7.

2.8 | Multiscale/layer LRS prediction averaging

To develop a single LRS, we averaged the predictions of our 'All Scale Combinations' (with a delta AICc <10) LRSs by weighting individual surfaces by AICc weight. We rescaled all multiscale/layer LRS resistance values from 1 to 100 prior to our weighted averaging and rescaled the final averaged multiscale/layer LRS from 1 to 40 to match the LRS range used in Compton, McGarigal, Cushman, and Gamble (2007).

2.9 | Correlation in LRSs

We measured Spearman's rank correlation coefficient between the prediction-averaged AMMA and AMOP LRSs and the expert-derived LRS in Compton et al. (2007). We used the function rasterCorrelation from the R package spatialEco (Evans, 2017) to highlight where, in the study area, the AMMA and AMOP LRSs showed agreement and disagreement in LR value.

2.10 | Evaluating, scoring and identifying important VPs

We identified high quality and highly connected VPs for AMMA and AMOP by evaluating and scoring them based on the quality of surrounding upland habitat and the amount of connectivity with other VPs on the landscape at multiple spatial levels (local, neighbourhood and regional levels following Compton et al. (2007)). Our approach differed in that our resistant kernels (see below) were driven by an empirically optimized multiscale/layer LRS as compared to the expert-derived LRS used by Compton et al. (2007). Resistant kernels were fit to VPs using the R package gridprocess (https://github.com/ethanplunkett/gridprocess). R code to score and identify important VPs based on resistant kernels is available online (https://github.com/withakri/Vernal-Pool-Scoring).

2.11 | Local score

VP scores at the local level were determined by the intensity of forest land cover in 2005 within the ecological neighbourhood of each VP defined by a Gaussian kernel. The Gaussian kernel bandwidth *b* (*h*; the standard deviation of a bivariate normal curve) was 124 m, which was based on the 66th percentile of maximum migratory distances from VPs for 28 individual spotted salamanders (McDonough & Paton, 2007), as in Compton et al. (2007). We calculated the local score for each VP by summing the Gaussian weights of forested cells surrounding the pool and then rescaling those values from 1 to 10, with 10 as the highest score.

2.12 | Neighbourhood score

VP scores at the neighbourhood level reflect how well a VP is connected to neighbouring vernal pools. VP scores at the neighbourhood level were based on a Gaussian resistant kernel (Compton et al., 2007). Briefly, a Gaussian resistant kernel uses a multidirectional least-cost path algorithm that measures the functional distance from a focal cell to every neighbouring cell within a defined dispersal distance (Compton et al., 2007; Cushman, Lewis, & Landguth, 2014). Compton et al. (2007) used a bandwidth of approximately 400m, which was the standard deviation of a normal curve of dispersal distances from a study of AMOP dispersal distances among 14 vernal pools in our study area (Gamble et al., 2007). We increased the Gaussian resistant kernel bandwidth to 800 m because we found that a 400 m bandwidth did not adequately discriminate neighbourhood scores among VPs across our landscape. This was due to the LR values of our LRSs being higher on average than the values in Compton et al. (2007), limiting the spread of our Gaussian resistant kernels. We calculated the neighbourhood score for each VP by summing the resistant kernel value of neighbouring VPs overlapping the focal VP and then rescaling those values from 1 to 10, with 10 as the highest score.

2.13 | Regional score

VP scores at the regional level were determined by the total number of VPs within a VP 'cluster' (Compton et al., 2007). Clusters consisted of discrete overlapping neighbourhood kernels on the landscape and were identified using the function patch scan in the R package gridio. Briefly, we first applied a Gaussian resistant kernel similar to our neighbourhood Gaussian resistant kernel but increased the bandwidth (2,800 m for AMMA and 2,000 m for AMOPs) to better capture gene flow over multiple generations at a broader spatial scale. Selection of a kernel bandwidth for the regional score was more arbitrary as we wanted a bandwidth to capture multigenerational gene flow but that also had good discrimination across the range of our VPs. A bandwidth >2,000 m for AMOPs resulted in very large clusters of VPs, which did not allow us to distinguish regional scores among VPs in our landscape as all VPs received a high regional score. The same was not true for AMMAs, and we felt that a higher Gaussian kernel bandwidth could be justified for AMMA due to a larger body size that potentially allows for longer dispersal distances, thus higher regional connectivity (Denton, Greenwald, & Gibbs, 2017; Petranka, 1998). We calculated the regional score for each VP by counting the number of VPs in the 'cluster' containing the focal VP and then rescaling those values from 1 to 10, with 10 as the highest score.

To calculate a final species-specific score for each VP, we first rescaled each score (local, neighbourhood and regional) from 1 to 10 and then computed the geometric mean. We also measured the Spearman's rank correlation coefficient between the AMMA, AMOP and Compton et al. (2007) VP geometric mean scores.

3 | RESULTS

3.1 | Genetic differentiation and gene flow

Genetic differentiation among local VP populations (measured by D_C) was stronger with AMOPs than with AMMAs across our study area (Figure 3; Supporting Information S6 and S7). Whiteley et al.

(2014) identified three population-level clusters of VPs sampled for AMOPs and only 1 population-level cluster for AMMAs, indicating landscape features were likely limiting gene flow more for AMOPs than for AMMAs. AMMA exhibited a weaker linear increase in genetic differentiation with increasing geographic distance (Figure 3) (see Whiteley et al. (2014) for more detail regarding genetic differentiation among populations for AMMAs and AMOPs).

3.2 | Multiscale/single-layer LRSs

The single-layer LRS that best described genetic pattern and inferred gene flow for AMMAs based on AICc was our most recent temporal representation of forest land cover (2005) (Figure 4). Forest land cover in 2005 was optimized with a reverse monomolecular transformation, 1.66 shape and 259 maximum resistance value, and with forest land cover smoothed using a 500-m bandwidth Gaussian kernel. Resistance increased with decreasing forest land cover. Top surfaces based on AICc also included LRSs derived from NDVI (500-m bandwidth) and impervious surface (500-m bandwidth) spatial layers (Figure 4). The single-layer LRS that best described genetic pattern and inferred gene flow for AMOPs based on AICc was traffic rate (Figure 4). Traffic rate was optimized with a monomolecular transformation, 0.08 shape and 180 maximum resistance value, and with traffic rate smoothed using a 500-m bandwidth Gaussian kernel. Resistance increased with increasing traffic rate, although resistance asymptotically approached its maximum value at relatively low traffic rates. Topographic curvature (1,000-m bandwidth) and impervious surface (500-m bandwidth) LRSs also performed well in describing the genetic pattern and differentiation of AMOP (Figure 4). Surprisingly, LRSs optimized using the VP spatial layer performed poorly for both species at all spatial scales (Figure 4). More recent representations of forest land cover (2005) performed better than past representations of forest land cover for both AMMAs and AMOPs (Figure 4). LRSs modelled at the original 60-m spatial scale performed relatively poorly compared to the smoothed layers for both species (Figure 4). For example, the best supported spatial layer for AMOP (traffic rate at a 500-m bandwidth) was > 9 AICc units better than traffic rate at the original 60-m spatial scale, and forest land cover (2005) at 500-m bandwidth was > 10 AICc units better than forest land cover at the original 60-m scale (Figure 4). TWI for AMOPs was the only LRSs, which performed better at the original spatial scale based on AICc (Figure 4).

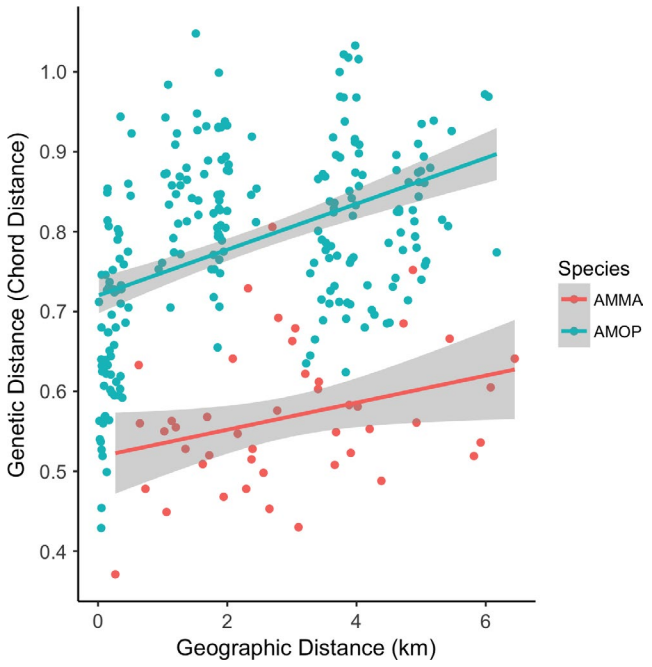

FIGURE 3 Genetic distance (chord distance; DC) vs. geographic distance (km) for spotted (Ambystoma maculatum) and marbled (A. opacum) salamanders in the Pioneer Valley in western Massachusetts. DC values for both species are based on a subset of the data with one randomly sampled full-sibling per family from all vernal pools. Two A. maculatum and seven A. opacum vernal pools that contained 10 or fewer full-sib families were removed prior to the calculation of genetic distance. A linear regression and 95% CI were fit to A. maculatum and A. opacum genetic distance data and shown here

3.3 | Multiscale/layer LRSs

The multiscale/layer LRSs derived by fitting spatial layers at their optimized spatial scale did not perform better than single-layer LRSs at their optimized spatial scale. For example, with AMMA, an LRS optimized from forest land cover (500m) had an AICc value 0.57 less than a LRS optimized from both forest land cover (500 m) and NDVI (500m). Similarly, with AMOP, an LRS optimized from traffic rate (500 m) had an AICc value 0.32 less than a LRS optimized from both topographic curvature (1,000 m) and traffic rate (500 m). However, LRSs derived from 'All Scale Combinations' of the top two performing single-layer LRSs performed better than the single-layer LRSs and the multiscale/layer pseudo-optimized bandwidth combinations. For AMMA, the top model included forest land cover (2005) smoothed using a 500-m bandwidth Gaussian kernel and NDVI smoothed using a 100-m bandwidth Gaussian kernel (R2m = 0.38; Supporting Information S6). For this model, resistance decreased with increasing forest land cover, optimized with a reverse monomolecular transformation and 1.88 shape and 490 maximum resistance value, and decreased with increasing NDVI, optimized with a reverse monomolecular transformation and 1.54 shape and 470 maximum resistance value (Figure 5). For AMOP, the top model included traffic rate and topographic curvature, both smoothed using 500-m bandwidth Gaussian kernels (R2m = 0.44; Supporting Information S7). For this model, resistance increased rapidly with increasing traffic rate, optimized with a monomolecular transformation and 0.21 shape and 237 maximum resistance value, and increased with topographic curvature, optimized with a monomolecular transformation and 1.08 shape and 250 maximum resistance value (Figure 5).

3.4 | Multiscale/layer LRS averaging

The averaged LRS from the multiscale/two-layer 'All Scale Combinations' LRS showed high resistance for AMMA in nonforested areas and high resistance for AMOP within the vicinity of roads and in areas on the landscape with high topographic curvature (Figure 6).

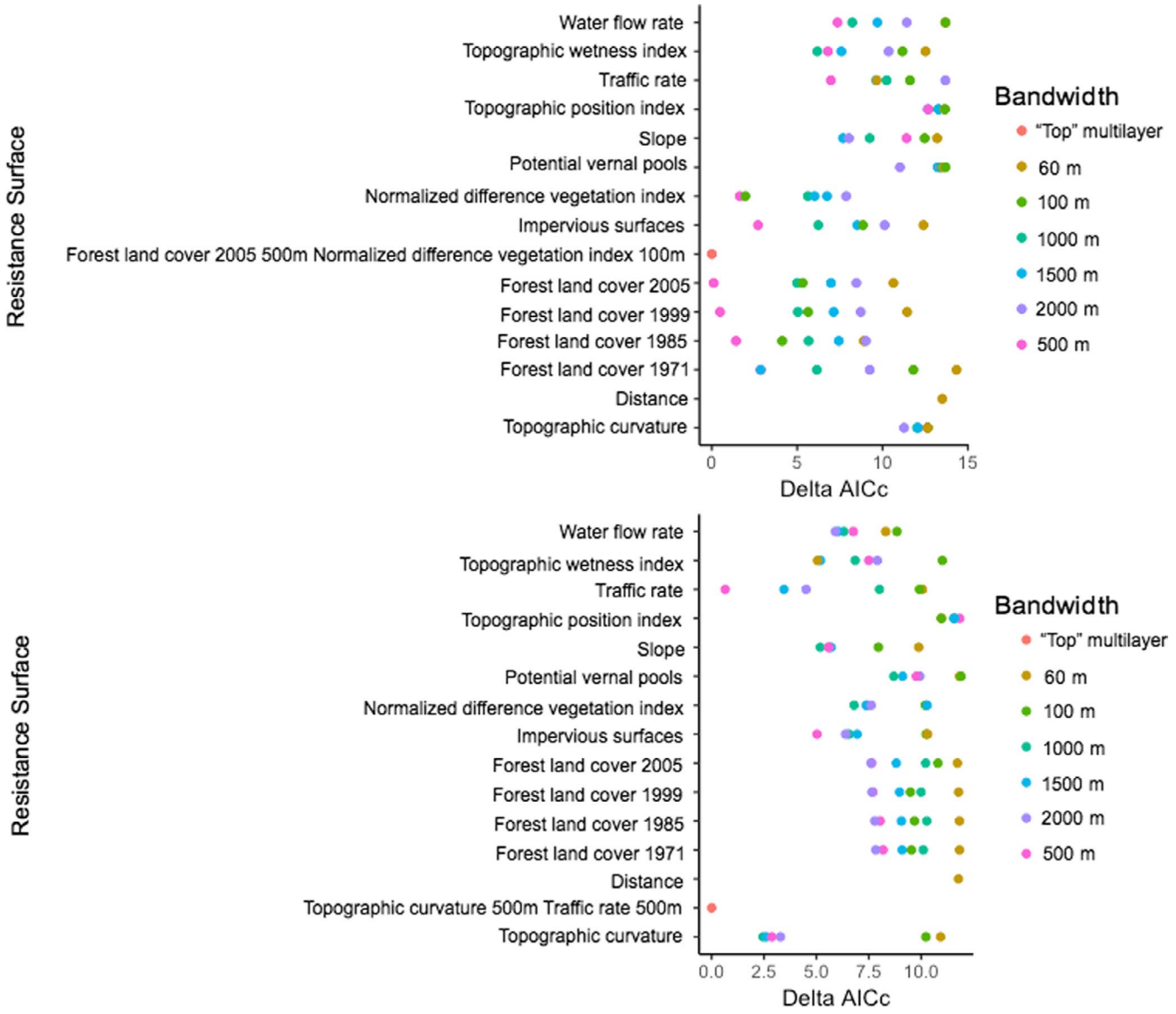

FIGURE 4 Akaike's information criteria corrected for small sample sizes (AICc) for single-layer landscape resistance models, which were optimized at the original pixel size (60 m) and different Gaussian kernel bandwidths (100 m, 500 m, 1,000 m, 1,500 m and 2,000 m) for spotted (Ambystoma maculatum; top panel) and marbled (A. opacum; bottom panel) salamanders. Also included is the AICc of the "top" multilayer resistance surface

3.5 | Patterns of LRSs differed by species and estimation method used to estimate resistance

Correlation between the AMOP and AMMA LRSs was moderate (Spearman's rank correlation coefficient = 0.70) with the different species-specific drivers (modelled at different spatial scales) of LR resulting in areas of agreement and disagreement in values across the study area (Supporting Information S10). Correlation was higher between the AMMA LRS and the Compton et al. (2007) expert-derived LRS (Spearman's rank correlation coefficient = 0.70) than between the AMOP LRS and the Compton et al. (2007) expert-derived LRS (Spearman's rank correlation coefficient = 0.43) (Supporting Information S8).

3.6 | VP scores

Local scores were high for VPs outside the Pioneer Valley where the land cover is dominated by forest (Figure 7). Neighbourhood scores for AMMAs were highest in portions of the study area with low LR and high VP densities, which occurred in the western portion of the study area and in the Holyoke range (Figure 7). Neighbourhood scores for AMOPs were also highest in portions of the study area with low LR and high VP densities, which occurred in the portion of the study area east of the Connecticut River (Figure 7). Regional scores for AMMA were highest in a handful of VP clusters on both the west and east side of the Connecticut River, whereas regional scores for AMOPs were highest mainly on the east side of the

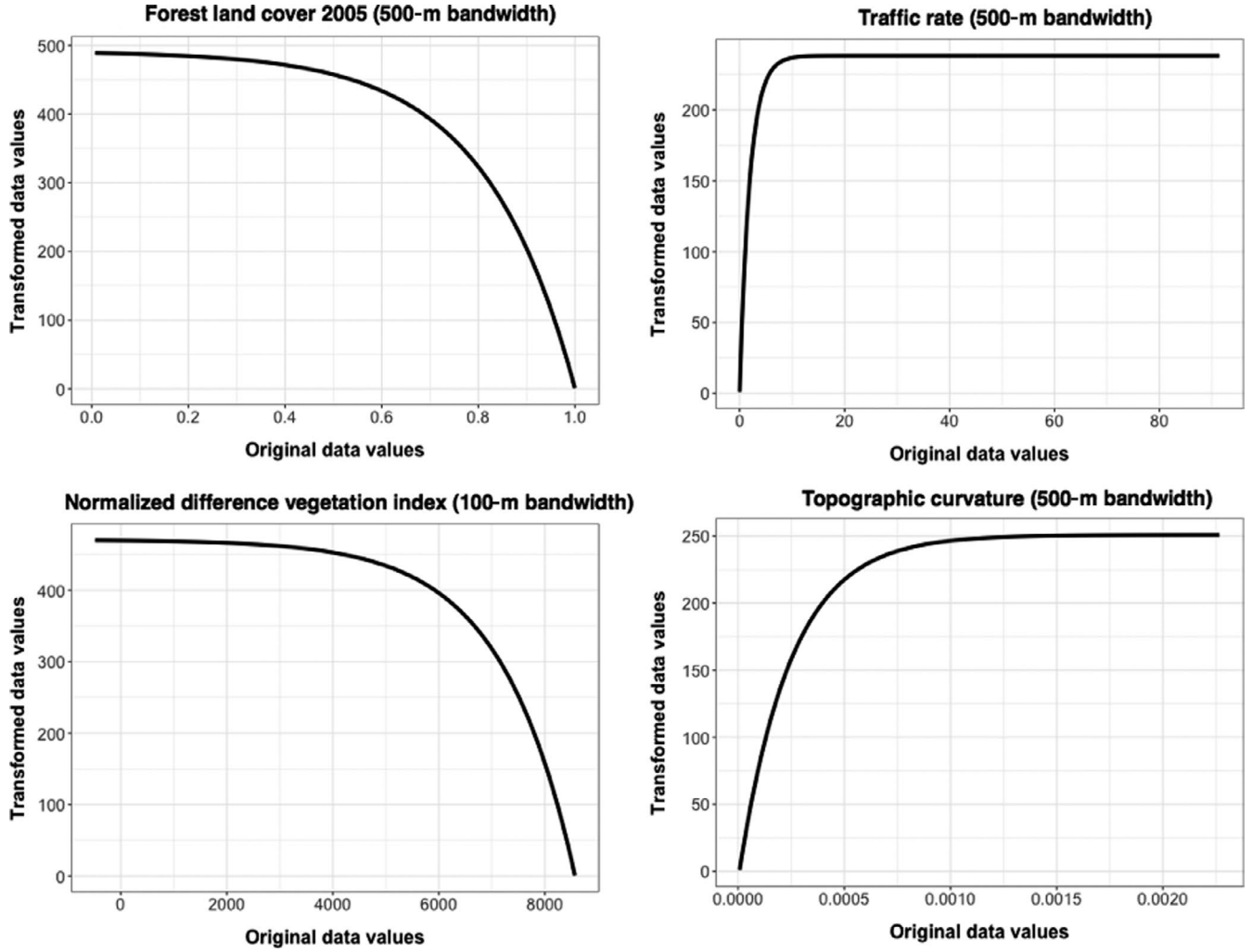

FIGURE 5 Response curves demonstrating the multiscale/layer contribution and relationship of forest land cover at 2005 (500-m Gaussian kernel bandwidth) and normalized difference vegetation index (100-m Gaussian kernel bandwidth) to landscape resistance for spotted salamanders (Ambystoma maculatum; left panels) and traffic rate (500-m Gaussian kernel bandwidth) and topographic curvature (500-m Gaussian kernel bandwidth) to landscape resistance for marbled salamanders (A. opacum; right panels)

Connecticut River (Figure 7). Overall scores (i.e. geometric mean of local, neighbourhood and regional scores) for AMMAs were highest in multiple clusters of VPs in largely forested regions of our study area, which included the Holyoke Range and areas west and east of the Pioneer Valley (Figure 8). Overall scores for AMOP were highest in clusters of VPs in areas of low topographic curvature and away from roads in our study area, which occurred more in the eastern portion of the study area (Figure 8). In contrast to the moderate correlation patterns found between the AMMA and AMOP LRSs, correlation between the AMMA and AMOP VP scores was relatively low (Spearman's rank correlation coefficient = 0.43) (Supporting Information S9). Similar to the patterns observed for LRSs, correlation was higher between the AMMA and the Compton et al. (2007) VP scores due to overall similarities in LRSs (Spearman's rank correlation coefficient = 0.70) than between the AMOP and the Compton et al. (2007) VP scores (Spearman's rank correlation coefficient = 0.47) (Supporting Information S9 and S10).

4 | DISCUSSION

Our research adds to the growing number of ecological disciplines and analyses successfully incorporating a multiscale evaluation of relevant environmental and anthropogenic predictors (McGarigal et al., 2016) and highlights the benefits of such an approach when optimizing LR. More specifically, our study resulted in the following major findings. Our multiscale/layer LRSs empirically optimized using ResistanceGA performed better than LRSs derived from spatial layers at their original spatial scale and revealed different possible environmental and anthropogenic predictors of genetic pattern and inferred gene flow for these two ecologically similar species. Our focal organisms, VP-breeding salamanders, also provided a study case in which genetic connectivity was constrained by the spatial configuration of the local populations across the landscape. Resistant kernels allowed us to (i) model this connectivity between a VP and its surrounding uplands and among VPs at neighbourhood and regional scales based on empirical

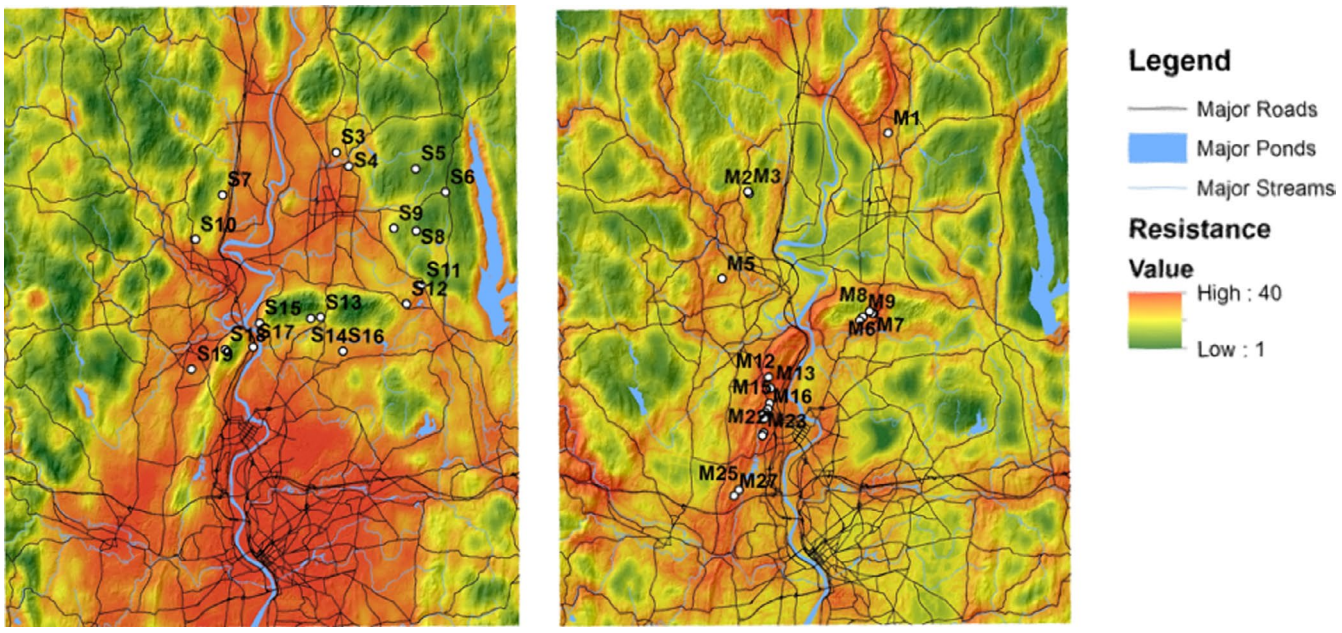

FIGURE 6 Landscape resistance surfaces derived from the predicted averages of the top "All Scale Combinations" multiscale/two-layer surfaces for spotted (Ambystoma maculatum; left panel) and marbled (A. opacum; right panel) salamanders

dispersal data, and (ii) score VPs based on this connectivity at multiple levels to better inform conservation of VPs in our study area.

4.1 | LRSs accounting for ecological neighbourhood perform best

Multiscale LRSs empirically optimized using ResistanceGA performed better than LRSs derived from spatial layers at their original spatial scale, demonstrating the importance of considering ecological neighbourhood size (sensu Addicott et al., 1987) when deriving LRSs. Moreover, LRSs optimized with spatial layers smoothed at mid-scales (i.e. 100- to 500-m bandwidth Gaussian kernels) performed best. The optimization of mid-scale bandwidths is likely driven by the extent of our study area, the scale of habitat selection for these two species and to a lesser degree their known dispersal distance. For example, a bandwidth of 500 m for forest land cover suggests that AMMA select and prefer to disperse through moderate to large forested tracts of land, while an optimized bandwidth of 100 m for TWI suggests that topographic wetness is more important at the scale of just a few pixels. Species-specific differences between AMMA and AMOP in optimized bandwidth are likely due to ecological differences between the two species. The pseudo-optimized Gaussian kernel bandwidth for forest land cover was 500 m for AMMA, but was 2000 m for AMOP. These differences might suggest that AMOP gene flow is greater in portions of the landscape with more forested land cover. However, forest land cover was not found to meaningfully influence AMOP gene flow and differentiation. Our findings are generally consistent with a recent multiscale exploration of gene flow in Pumas (*Puma concolor*), which found that larger (up to 6,000 m) Gaussian kernel bandwidths were optimal. These findings align with life history differences between Pumas and our focal species, with Pumas having larger home range size and greater dispersal ability (Zeller et al., 2017). It is important to note that if we had only evaluated surfaces at their original scale, our best supported AMOP LRS would have been topographic wetness index and our best supported AMMA LRS would have been forest land cover (1985). This would have resulted in much different spatial patterns of LR, overall interpretation of species-specific LR and VP scores at the neighbourhood and regional level.

4.2 | Environmental and anthropogenic spatial predictors of landscape resistance

Optimized multiscale/layer LRSs revealed possible different environmental and anthropogenic predictors of genetic pattern and inferred gene flow for our two ecologically similar focal species. Environmental and anthropogenic predictors of LR and the species-specific differences were mostly in agreement with recent landscape genetics findings with VP-breeding amphibians and other taxa. Our AMMA multiscale/layer LRS showed decreased resistance with increasing forest land cover (smoothed at 500 m) and a finer scale measure of land cover type (as proxied by NDVI smoothed at 100 m) and is consistent with several studies that have found reduced forest land cover and increased agriculture and residential development associated with increased population isolation and reduced gene flow with amphibians (Greenwald, Gibbs, & Waite, 2009; Greenwald, Purrenhage, & Savage, 2009; Spear & Storfer, 2008). Our AMOP multiscale/layer LRS reflecting high resistance at relatively low traffic rates and increased resistance with topographic complexity (or curvature) is also consistent with other amphibian landscape genetics

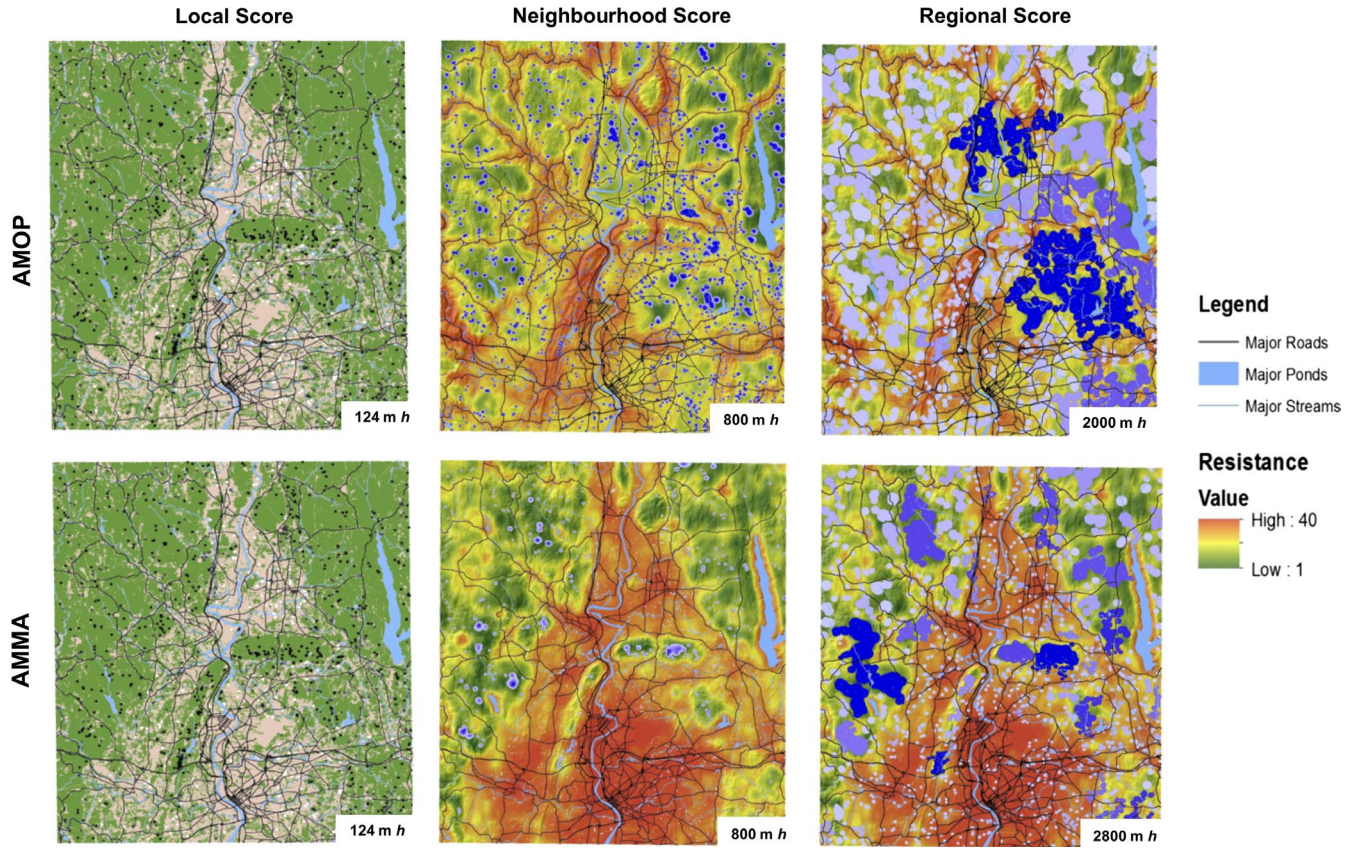

FIGURE 7 Local (left panel), neighbourhood (middle panel) and regional scores (right panel) for marbled (Ambystoma opacum; top row) and spotted (A. maculatum; bottom row) salamanders. Local vernal pool scores were derived by summing the Gaussian kernel volume of forest land cover cells (2005) based on a Gaussian kernel (124-m bandwidth) centred on each vernal pool in the study area. Low scoring local vernal pools are represented in white, and high scoring pools are represented in black. Neighbourhood vernal pool scores were derived by summing the volume of neighbouring vernal pools based on a Gaussian kernel (800-m bandwidth) resistant kernel volumes. Low scoring neighbourhood vernal pools are represented in light blue with high scoring vernal pools in dark blue. Regional vernal pool scores were derived by summing the total number of vernal pools within each resistant kernel "cluster" (2,800-m bandwidth for AMMA and 2,000-m bandwidth for AMOP). Low scoring regional vernal pool "clusters" are light blue, and high scoring vernal pool "clusters" are dark blue

studies (Coster, Babbitt, Cooper, & Kovach, 2015; Richardson, 2012; Zellmer & Knowles, 2009).

We were surprised with our optimized LRS for AMOP by the high resistance in the forested portions of our study area with high topographic curvature, as we expected that some of these areas were comprised of more intact habitat in our study area for VP-breeding salamanders. This suggests that AMOPs potentially cannot disperse well in rugged terrain despite high forest cover, which is in agreement with other studies showing that topography can influence genetic structure (Funk et al., 2005; Giordano, Ridenhour, & Storfer, 2007; Murphy, Dezzani, Pilliod, & Storfer, 2010). It is worth noting that VPs M16 to M21 did exhibit high levels of gene flow in what our LRS predicts as having high resistance due to high topographic curvature, but these VPs were close proximity (mean pairwise Euclidean distance = 387m; Whiteley et al., 2014) when compared to observed AMOP dispersal distances (up to 1,300 m; Gamble et al., 2007). Less surprising was the observed high resistance to inferred gene flow by roads for AMOP. High resistance to gene flow caused by roads has been well documented with many taxa (Balkenhol & Waits, 2009; Jackson & Fahrig, 2016) and has been previously documented in VP-breeding amphibians (Coster et al., 2015; Richardson, 2012). Roads have been found to cause population declines with VP-breeding amphibians due to direct mortality, and VPs close to roads which are treated (e.g. salted) have been found to have reduced fecundity (Gibbs & Shriver, 2005; Karraker, Gibbs, & Vonesh, 2008). Surprisingly, we did not find a steady increase in LR with increasing traffic rate, which has been documented in other taxa (Shirk et al., 2010). Instead, we observed more of an all or nothing response to roads (Figure 5). This could suggest that just the physical barrier of a narrow single lane road may be enough to impede gene flow of salamanders than the higher levels of direct mortality of adults and juvenile salamanders found with multilane roads (e.g. interstate highways) or that roads are correlated with an unknown spatial feature of the landscape. In contrast to roads and our expectations, we found that the Connecticut River, a large river bisecting the study area, did not significantly reduce inferred gene flow, which contradicts findings that rivers and other large water bodies are important natural impediments to gene flow for VP-breeding amphibians (Coster et al., 2015; Richardson, 2012).

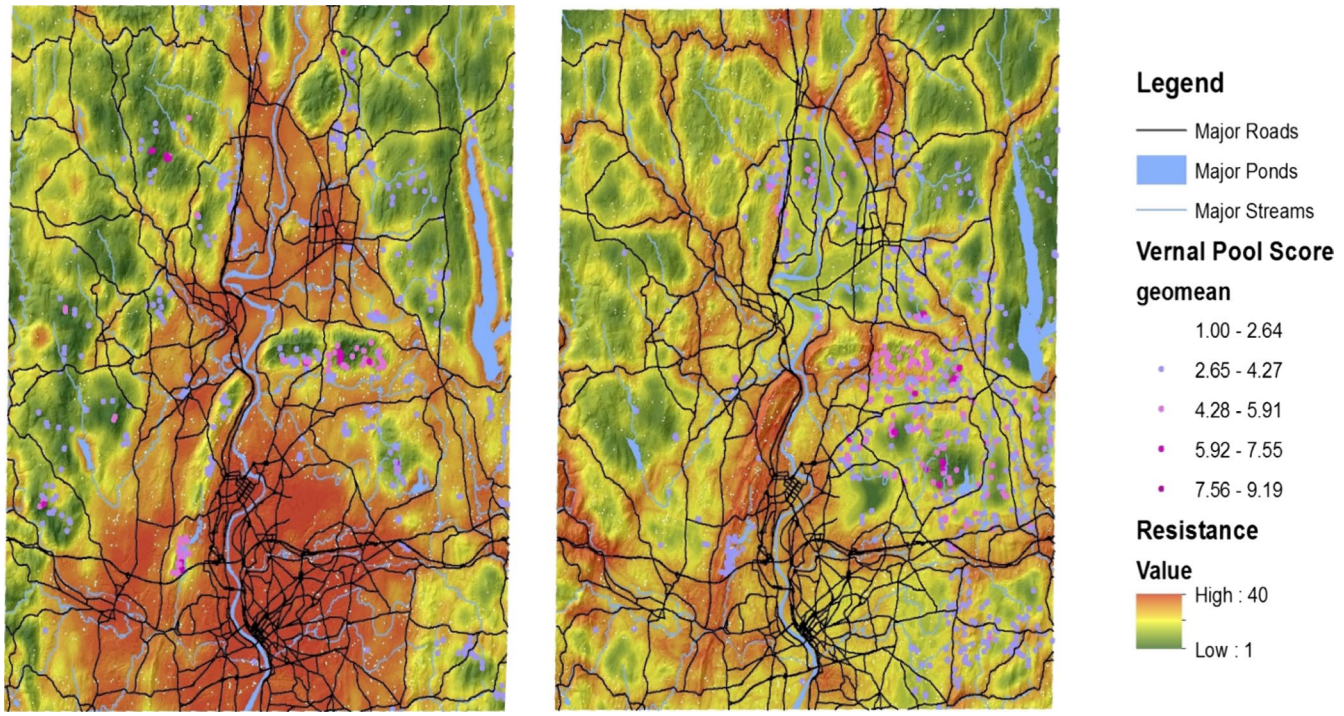

FIGURE 8 Final vernal pool scores for Ambystoma maculatum (left panel) and A. opacum (right panel) were calculated by taking the geometric mean of the local, neighbourhood and regional scores

4.3 | Recent landscapes best describe gene flow

Multidecadal temporal snapshots of land cover imagery for our study area allowed us to explore which temporal snapshot of our landscape best described the present genetic patterns and inferred gene flow. Our results support recent studies that have found shorter time lags between landscape composition and genetic distance than expected based on species generation length (Draheim, Moore, Fortin, & Scribner, 2018), as we found that the most recent forest land cover (2005) spatial layer best described the genetic pattern and inferred gene flow of both AMMA and AMOPs (5 years prior to AMMA sampling and 2–3 years prior to AMOP sampling). Indeed, for both species, forest land cover from 1971 performed poorest compared to forest land cover from 1985 and 1999. This suggests that these species' gene flow and genetic patterns rapidly adjust to changes in landscape structure, and is likely a function of recent environmental conditions that would support gene flow across the landscape (e.g. optimal VP hydrology) (Mui, Caverhill, Johnson, Fortin, & He, 2017; Watts et al., 2015).

4.4 | Population-level genetic clustering and gene flow with ecologically similar species

We observed significant differences between AMMA and AMOP with regard to population-level clustering across the landscape and with the environmental and anthropogenic features best predicting gene flow, which is consistent with previous studies comparing the landscape genetics of ecologically similar species (Burkhart et al., 2017; Coster et al., 2015; Goldberg & Waits, 2010; Peterman et al., 2015; Richardson, 2012; Steele, Baumsteiger, & Storfer, 2009). AMMA had no evidence of population-level clustering, a relatively weak pattern of isolation by distance, and little variation in family-level genetic structure (Whiteley et al., 2014), and this is consistent with past AMMA studies (Burkhart et al., 2017; Coster et al., 2015; Peterman et al., 2015; Purrenhage, Niewiarowski, & Moore, 2009; Richardson, 2012). In contrast, AMOP showed population-level clustering and stronger patterns of isolation by distance and variation in family genetic structure, which is also consistent with past AMOP studies (Burkhart et al., 2017; Peterman et al., 2015). These findings are likely the result of differences in AMMA and AMOP life histories, phenology and morphology. For example, AMMAs are likely able to disperse further across the landscape compared with AMOPs due to their larger body size, although AMMA on average likely disperse shorter distances due to the fact they are able to breed in a broader range of VPs across the landscape due to a greater flexibility in VP hydroperiod requirements (Burkhart et al., 2017; Gamble et al., 2007; Peterman et al., 2015). Burkhart et al. (2017) hypothesized that differences in breeding phenology (AMOP breed in fall while AMMA breed in spring) likely allow spring breeding salamanders to breed in a wider range of VP hydroperiods and to be more opportunistic in breeding pond use. In doing so, AMMA likely has reduced natal philopatry compared with the fall breeding AMOP. AMMA also have much larger effective population sizes (N_b) than AMOP (AMMA N_b = 422 ± 122 SE, AMOP N_b = 96 ± 47) (Whiteley et al., 2014) and longer generation length (Petranka, 1998).

4.5 | Identifying important VPs on the landscape

Our resistant kernel approach allowed us to identify highly connected VPs in our study area with high amounts of local forested habitat, although further effort will be needed to assess finer scale VP characteristics and species-specific occupancy and/or abundance. VP hydroperiod, chemistry (e.g. conductivity), microhabitat characteristics (e.g. logs), and tree species composition are known to be important drivers of species presence/abundance (Charney, 2011) and were not included in our VP scoring at local, neighbourhood, or regional levels. Recent evidence also suggests that VPs that have higher productivity have higher rates of gene flow, which would result in differences in scores at the neighbourhood and regional level (Coster et al., 2015; Murphy et al., 2010).

Our empirically based final VP scores differed somewhat from the expert-based scores of Compton et al. (2007), suggesting the importance of using empirical approaches when available, and this is consistent with other studies that have demonstrated superior performance of empirical approaches over expert-opinion approaches (Mateo-Sánchez et al., 2015; Shirk, Schroeder, Robb, & Cushman, 2015; Wasserman, Cushman, Schwartz, & Wallin, 2010; Zeller et al., 2018). However, it is worth noting that our empirically based VP scores were not directly comparable to the expert-based scores of Compton et al. (2007), as the latter were not species-specific. Nevertheless, the Compton et al. (2007) VP scores were more similar to our AMMA VP scores than our AMOP VP scores, perhaps reflecting greater familiarity with AMMA among the regional experts as it is a more common and better studied species.

It is also worth noting that our spatial data set of VPs is limited to potential VPs that have not been field verified. A comprehensive field verified data set does exist, but the spatial distribution of certified VPs is biased to those areas on the landscape under consideration for residential/commercial development. Also, since potential VPs are based off of imagery, smaller VPs are likely missing from this spatial layer. This spatial layer also includes no information on VP quality which we know is driven by factors such as hydroperiod, with species preference often differing with hydroperiod (Peterman et al., 2014; Semlitsch, Peterman, Anderson, Drake, & Ousterhout, 2015). Upland forest composition and age may also be a factor in determining VP quality, but was not incorporated in scoring of VPs at the local level in our study, although a recent study found no effect of forestry practices on VP amphibian gene flow (Coster et al., 2015).

4.6 | Assumptions and limitations

Our findings are subject to a couple of noteworthy assumptions and limitations. First, our multiscale/layer LRS approach did not allow us to fully explore all spatial layer/bandwidth combinations due to the excessive computational demands of ResistanceGA's genetic algorithm optimization. To successfully fit models at the spatial extent of our landscape, we were required to coarsen our original 30 m × 30m pixels to 60 m × 60 m pixels, thus sacrificing potentially important fine-scale information about landscape patterns. Although coarsening cell resolution has been found to have minimal impact on inferences in this context (Cushman & Landguth, 2010; McRae et al., 2008) and given that the top performing models were comprised of spatial layers smoothed at 100–500 m, the coarsening may not have been consequential in this case. In addition, to represent ecological neighbourhoods at varying spatial scales, we pseudo-optimized the neighbourhood scale for each layer by evaluating a predetermined and limited number of neighbourhood sizes (i.e. Gaussian kernel bandwidths). This approach did not allow us to identify the very best neighbourhood scale on a continuum of possibilities but represented a reasonable trade-off between finding the best scale and computational feasibility. In addition, we were unable to fit complex multilayer models involving more than two or three layers due to computational deficiencies in the data and the challenges of optimization in a higher dimensional parameter space. We deemed this limitation acceptable and better than alternative analysis frameworks reliant on less rigorous searches of parameter space or questionable statistical models (Peterman et al., 2019), but recognize that overcoming this partly technical limitation should be a focus of future work. Indeed, the inability to fully optimize the neighbourhood scale in complex multilayer models is potentially a serious shortcoming. Recall that our two-stage approach of pseudo-optimizing spatial layers at their 'best' spatial scale and then developing multilayer LRSs performed poorer than our single-layer LRSs, and we attributed this to the high correlation between spatial surfaces optimized at similar kernel bandwidths (Supporting Information S2 and S3). Our two-layer models evaluated across all combinations of the predetermined and limited number of scales resulted in significantly better models, highlighting the importance of a fully multiscale/layer optimization. The most recent version of ResistanceGA includes optimization of Gaussian kernel bandwidth within the genetic algorithm, which makes possible full multiscale/layer optimization. However, our preliminary examination of this capability suggests that there are still some major technical challenges to overcome for large data sets involving multiple spatial layers. Overcoming these technical challenges remains a priority of future work. A full optimization of resistance surfaces may also be unfeasible with very large landscapes using ResistanceGA due to current computational limitations. Here, a pseudo-optimization approach (Shirk et al., 2010) may be more feasible, although this approach has its own set of unique challenges and has been found to have high type I error rates with multivariate simulations (Peterman et al., 2019).

Second, we used Gaussian resistant kernels (Compton et al., 2007) to compute neighbourhood and regional connectivity scores for VPs. The resistant kernel bandwidth we used was difficult to select because we did not know what the dispersal kernel would be on a nonresistant landscape. Our chosen 800-m bandwidth at the neighbourhood scale may have underestimated dispersal distance in a nonresistant landscape. Similarly, the selection of the bandwidth for the regional connectivity scoring was somewhat arbitrary because it reflected a temporal component regarding connectivity over multiple generations. We simply selected a bandwidth that gave us a distribution of VP scores that allowed us to discriminate among VPs at the study area level.

Lastly, the measures of genetic distances used as the response variable to model LR in our study are assumed to be driven completely by LR. It is likely that population demographics and genetic drift also affect measures of genetic distance between populations (Prunier, Dubut, Chikhi, & Blanchet, 2017), which has potential to bias our LRS models and subsequently our neighbourhood and regional VP scores. However, MLPE models appear to absorb and account for much of these drift-based discrepancies (W.E. Peterman, unpublished data). We were conservative with the inclusion of populations in our study area used to estimate genetic distance by filtering out populations with low estimates of unique full-sibling families to minimize issues associated with genetic drift.

5 | CONCLUSIONS

Our findings confirm that multiscale approaches (in combination with multiple spatial layers) are not only feasible but can result in improved models of species–environment relationships (McGarigal et al., 2016), and thus should be considered in all future studies optimizing LR. Our findings also confirm previous multispecies comparisons, which have shown that we should not assume that ecologically similar species have comparable rates of gene flow and genetic differentiation and that it is incorrect to assume that environmental and anthropogenic predictors of landscape resistance for those species are the same (Burkhart et al., 2017; Richardson, 2012). Thus, management practices geared towards the conservation of one species may not be beneficial for other assumed ecologically similar species. Species-specific resistant kernels derived from our multiscale LRS allowed us to score VPs across our study area based on genetic connectivity and highlight an approach that we feel could be applicable to the conservation of wide range of taxa beyond VP-breeding salamanders.

ACKNOWLEDGEMENTS

We thank B. Compton, M. Chesser and J. Estes for salamander sample collection and J. Estes, S. Jane, A. Pant and K. Pilgrim for genetic data collection. E. Plunkett assisted with using his R packages gridkernel and gridprocess and with optimizing LRSs on the UMass Landscape Ecology Computing Cluster.

AUTHOR CONTRIBUTIONS

K.M. and A.R.W. conceived and designed the study; K.J.W., W.E.P., K.M. and A.R.W. analysed the data; K.J.W. wrote the manuscript with contribution from all co-authors.

DATA ACCESSIBILITY

The AMMA and AMOP genetic distance data and relevant spatial layers used to model landscape resistance are openly available in a Dryad Repository at https://doi.org/10.5061/dryad.358c50t.

ORCID

Kristopher J. Winiarski https://orcid.org/0000-0002-2272-9770

REFERENCES

Addicott, J. F., Aho, J. M., Antolin, M. F., Padilla, D. K., Richardson, J. S., & Soluk, D. A. (1987). Ecological neighborhoods: Scaling environmental patterns. *Oikos*, *49*(3), 340. https://doi.org/10.2307/3565770

Akaike, H. (1998). A new look at the statistical model identification. In E. Parzen, K. Tanabe, & G. Kitagawa (Eds.), *Selected Papers of Hirotugu Akaike* (pp. 215–222). New York, NY: Springer. https://doi.org/10.1007/978-1-4612-1694-0_16

Balkenhol, N., & Waits, L. P. (2009). Molecular road ecology: Exploring the potential of genetics for investigating transportation impacts on wildlife. *Molecular Ecology*, *18*(20), 4151–4164. https://doi.org/10.1111/j.1365-294X.2009.04322.x

Bates, D., Mächler, M., Bolker, B., & Walker, S. (2015). Fitting linear mixed-effects models using lme4. *Journal of Statistical Software*, *67*(1), https://doi.org/10.18637/jss.v067.i01

Burkhart, J. J., Peterman, W. E., Brocato, E. R., Romine, K. M., Willis, M. M. S., Ousterhout, B. H., … Eggert, L. S. (2017). The influence of breeding phenology on the genetic structure of four pond-breeding salamanders. *Ecology and Evolution*, *7*(13), 4670–4681. https://doi.org/10.1002/ece3.3060

Chambers, C. L., Cushman, S. A., Medina-Fitoria, A., Martínez-Fonseca, J., & Chávez-Velásquez, M. (2016). Influences of scale on bat habitat relationships in a forested landscape in Nicaragua. *Landscape Ecology*, *31*(6), 1299–1318. https://doi.org/10.1007/s10980-016-0343-4

Chandler, R., & Hepinstall-Cymerman, J. (2016). Estimating the spatial scales of landscape effects on abundance. *Landscape Ecology*, *31*(6), 1383–1394. https://doi.org/10.1007/s10980-016-0380-z

Charney, N. D. (2011). Movin' & Groovin' Salamanders: Conservation Implications of Large Scales and Quirky Sex, 148.

Clarke, R. T., Rothery, P., & Raybould, A. F. (2002). Confidence limits for regression relationships between distance matrices: Estimating gene flow with distance. *Journal of Agricultural, Biological, and Environmental Statistics*, *7*(3), 361–372. https://doi.org/10.1198/108571102320

Compton, B. W., McGarigal, K., Cushman, S. A., & Gamble, L. R. (2007). A resistant-kernel model of connectivity for amphibians that breed in vernal pools. *Conservation Biology*, *21*(3), 788–799. https://doi.org/10.1111/j.1523-1739.2007.00674.x

Coster, S. S., Babbitt, K. J., Cooper, A., & Kovach, A. I. (2015). Limited influence of local and landscape factors on finescale gene flow in two pond-breeding amphibians. *Molecular Ecology*, *24*(4), 742–758. https://doi.org/10.1111/mec.13062

Cushman, S. A., Elliot, N. B., Macdonald, D. W., & Loveridge, A. J. (2016). A multi-scale assessment of population connectivity in African lions (*Panthera leo*) in response to landscape change. *Landscape Ecology*, *31*(6), 1337–1353. https://doi.org/10.1007/s10980-015-0292-3

Cushman, S. A., & Landguth, E. L. (2010). Scale dependent inference in landscape genetics. *Landscape Ecology*, *25*(6), 967–979. https://doi.org/10.1007/s10980-010-9467-0

Cushman, S., Lewis, J., & Landguth, E. (2014). Why did the bear cross the road? Comparing the performance of multiple resistance surfaces and connectivity modeling methods. *Diversity*, *6*(4), 844–854. https://doi.org/10.3390/d6040844

Denton, R. D., Greenwald, K. R., & Gibbs, H. L. (2017). Locomotor endurance predicts differences in realized dispersal between sympatric sexual and unisexual salamanders. *Functional Ecology*, *31*(4), 915–926. https://doi.org/10.1111/1365-2435.12813

Draheim, H. M., Moore, J. A., Fortin, M.-J., & Scribner, K. T. (2018). Beyond the snapshot: Landscape genetic analysis of time series data reveal

responses of American black bears to landscape change. *Evolutionary Applications*, *11*(8), 1219–1230. https://doi.org/10.1111/eva.12617

Evans, J. S. (2017). spatialEco. R package version 0.0.1-7, doi: https://CRAN.R-project.org/package=spatialEco.

Funk, W. C., Blouin, M. S., Corn, P. S., Maxell, B. A., Pilliod, D. S., Amish, S., & Allendorf, F. W. (2005). Population structure of Columbia spotted frogs (*Rana luteiventris*) is strongly affected by the landscape. *Molecular Ecology*, *14*(2), 483–496. https://doi.org/10.1111/j.1365-294X.2005.02426.x

Gamble, L. R., McGarigal, K., & Compton, B. W. (2007). Fidelity and dispersal in the pond-breeding amphibian, *Ambystoma opacum*: Implications for spatio-temporal population dynamics and conservation. *Biological Conservation*, *139*(3–4), 247–257. https://doi.org/10.1016/j.biocon.2007.07.001

Gibbs, J. P., & Shriver, W. G. (2005). Can road mortality limit populations of pool-breeding amphibians? *Wetlands Ecology and Management*, *13*(3), 281–289. https://doi.org/10.1007/s11273-004-7522-9

Giordano, A. R., Ridenhour, B. J., & Storfer, A. (2007). The influence of altitude and topography on genetic structure in the long-toed salamander *(Ambystoma macrodactulym*). *Molecular Ecology*, *16*(8), 1625–1637. https://doi.org/10.1111/j.1365-294X.2006.03223.x

Goldberg, C. S., & Waits, L. P. (2010). Comparative landscape genetics of two pond-breeding amphibian species in a highly modified agricultural landscape. *Molecular Ecology*, *19*(17), 3650–3663. https://doi.org/10.1111/j.1365-294X.2010.04673.x

Grand, J., Buonaccorsi, J., Cushman, S. A., Griffin, C. R., & Neel, M. C. (2004). A multiscale landscape approach to predicting bird and moth rarity hotspots in a threatened pitch pine-scrub oak community. *Conservation Biology*, *18*(4), 1063–1077. https://doi.org/10.1111/j.1523-1739.2004.00555.x

Greenwald, K. R. (2010). Genetic data in population viability analysis: Case studies with ambystomatid salamanders. *Animal Conservation*, *13*(2), 115–122. https://doi.org/10.1111/j.1469-1795.2009.00339.x

Greenwald, K. R., Gibbs, H. L., & Waite, T. A. (2009). Efficacy of landcover models in predicting isolation of marbled salamander populations in a fragmented landscape. *Conservation Biology*, *23*(5), 1232–1241. https://doi.org/10.1111/j.1523-1739.2009.01204.x

Greenwald, K. R., Purrenhage, J. L., & Savage, W. K. (2009). Landcover predicts isolation in Ambystoma salamanders across region and species. *Biological Conservation*, *142*(11), 2493–2500. https://doi.org/10.1016/j.biocon.2009.05.021

Hanks, E. M., & Hooten, M. B. (2013). Circuit theory and model-based inference for landscape connectivity. *Journal of the American Statistical Association*, *108*(501), 22–33. https://doi.org/10.1080/01621459.2012.724647

Jackson, N. D., & Fahrig, L. (2016). Habitat amount, not habitat configuration, best predicts population genetic structure in fragmented landscapes. *Landscape Ecology*, *31*(5), 951–968. https://doi.org/10.1007/s10980-015-0313-2

Jenness, J. (2013). DEM surface tools. Jenness Enterprises,http://www.jennessent.com/arcgis/surface_area.htm

Johnson, C. J., Parker, K. L., Heard, D. C., & Gillingham, M. P. (2002). A multiscale behavioral approach to understanding the movements of woodland caribou. *Ecological Applications*, *12*(6), 1840–1860. https://doi.org/10.1890/1051-0761(2002)012[1840:AMBATU]2.0.CO;2

Johnson, D. H. (1980). The comparison of usage and availability measurements for evaluating resource preference. *Ecology*, *61*(1), 65–71. https://doi.org/10.2307/1937156

Karraker, N. E., Gibbs, J. P., & Vonesh, J. R. (2008). Impacts of road deicing salt on the demography of vernal pool-breeding amphibians. *Ecological Applications*, *18*(3), 724–734. https://doi.org/10.1890/07-1644.1

Krishnamurthy, R., Cushman, S. A., Sarkar, M. S., Malviya, M., Naveen, M., Johnson, J. A., & Sen, S. (2016). Multi-scale prediction of landscape resistance for tiger dispersal in central India. *Landscape Ecology*, *31*(6), 1355–1368. https://doi.org/10.1007/s10980-016-0363-0

Levin, S. A. (1992). The problem of pattern and scale in ecology: The robert H. MacArthur award lecture. *Ecology*, *73*(6), 1943–1967. https://doi.org/10.2307/1941447

Libiger, O., Nievergelt, C. M., & Schork, N. J. (2009). Comparison of genetic distance measures using human SNP genotype data. *Human Biology*, *81*(4), 389–406. https://doi.org/10.3378/027.081.0401

Manel, S., & Holderegger, R. (2013). Ten years of landscape genetics. *Trends in Ecology & Evolution*, *28*(10), 614–621. https://doi.org/10.1016/j.tree.2013.05.012

Manel, S., Schwartz, M. K., Luikart, G., & Taberlet, P. (2003). Landscape genetics: Combining landscape ecology and population genetics. *Trends in Ecology & Evolution*, *18*(4), 189–197. https://doi.org/10.1016/S0169-5347(03)00008-9

Mateo-Sánchez, M. C., Balkenhol, N., Cushman, S., Pérez, T., Domínguez, A., & Saura, S. (2015). A comparative framework to infer landscape effects on population genetic structure: Are habitat suitability models effective in explaining gene flow? *Landscape Ecology*, *30*(8), 1405–1420. https://doi.org/10.1007/s10980-015-0194-4

McDonough, C., & Paton, P. W. C. (2007). Salamander dispersal across a forested landscape fragmented by a golf course. *Journal of Wildlife Management*, *71*(4), 1163–1169. https://doi.org/10.2193/2006-380

McGarigal, K., Wan, H. Y., Zeller, K. A., Timm, B. C., & Cushman, S. A. (2016). Multi-scale habitat selection modeling: A review and outlook. *Landscape Ecology*, *31*(6), 1161–1175. https://doi.org/10.1007/s10980-016-0374-x

McRae, B. H., Dickson, B. G., Keitt, T. H., & Shah, V. B. (2008). Using circuit theory to model connectivity in ecology, evolution, and conservation. *Ecology*, *89*(10), 2712–2724. https://doi.org/10.1890/07-1861.1

Meirmans, P. G., & Tienderen, P. H. V. (2004). genotype and genodive: Two programs for the analysis of genetic diversity of asexual organisms. *Molecular Ecology Notes*, *4*(4), 792–794. https://doi.org/10.1111/j.1471-8286.2004.00770.x

Mui, A. B., Caverhill, B., Johnson, B., Fortin, M.-J., & He, Y. (2017). Using multiple metrics to estimate seasonal landscape connectivity for Blanding's turtles (*Emydoidea blandingii*) in a fragmented landscape. *Landscape Ecology*, *32*(3), 531–546. https://doi.org/10.1007/s10980-016-0456-9

Murphy, M. A., Dezzani, R., Pilliod, D. S., & Storfer, A. (2010). Landscape genetics of high mountain frog metapopulations. *Molecular Ecology*, *19*(17), 3634–3649. https://doi.org/10.1111/j.1365-294X.2010.04723.x

Peterman, W. E. (2018). ResistanceGA: An R package for the optimization of resistance surfaces using genetic algorithms. *Methods in Ecology and Evolution*, *9*(6), 1638–1647. https://doi.org/10.1111/2041-210X.12984

Peterman, W. E., Anderson, T. L., Ousterhout, B. H., Drake, D. L., Semlitsch, R. D., & Eggert, L. S. (2015). Differential dispersal shapes population structure and patterns of genetic differentiation in two sympatric pond breeding salamanders. *Conservation Genetics*, *16*(1), 59–69. https://doi.org/10.1007/s10592-014-0640-x

Peterman, W., Brocato, E. R., Semlitsch, R. D., & Eggert, L. S. (2016). Reducing bias in population and landscape genetic inferences: The effects of sampling related individuals and multiple life stages. *PeerJ*, *4*, e1813. https://doi.org/10.7717/peerj.1813

Peterman, W. E., Connette, G. M., Semlitsch, R. D., & Eggert, L. S. (2014). Ecological resistance surfaces predict fine-scale genetic differentiation in a terrestrial woodland salamander. *Molecular Ecology*, *23*(10), 2402–2413. https://doi.org/10.1111/mec.12747

Peterman, W. E., Winiarski, K. J., Moore, C. E., Carvalho, C. D. S., Gilbert, A. L., & Spear, S. F. (2019). A comparison of popular approaches to optimize landscape resistance surfaces. *Landscape Ecology*, https://doi.org/10.1007/s10980-019-00870-3

Petranka, J. W. (1998). *Salamanders of the United States and Canada*. Washington, DC: Smithsonian Institution Press.

Prunier, J. G., Dubut, V., Chikhi, L., & Blanchet, S. (2017). Contribution of spatial heterogeneity in effective population sizes to the

variance in pairwise measures of genetic differentiation. *Methods in Ecology and Evolution*, *8*(12), 1866–1877. https://doi.org/10.1111/2041-210X.12820

Purrenhage, J. L., Niewiarowski, P. H., & Moore, F.-B.-G. (2009). Population structure of spotted salamanders (*Ambystoma maculatum*) in a fragmented landscape. *Molecular Ecology*, *18*(2), 235–247. https://doi.org/10.1111/j.1365-294X.2008.04024.x

Richardson, J. L. (2012). Divergent landscape effects on population connectivity in two co-occurring amphibian species. *Molecular Ecology*, *21*(18), 4437–4451. https://doi.org/10.1111/j.1365-294X.2012.05708.x

Richardson, J. L., Brady, S. P., Wang, I. J., & Spear, S. F. (2016). Navigating the pitfalls and promise of landscape genetics. *Molecular Ecology*, *25*(4), 849–863. https://doi.org/10.1111/mec.13527

Scrucca, L. (2013). **GA** : A Package for Genetic Algorithms in *R*. *Journal of Statistical Software*, *53*(4), https://doi.org/10.18637/jss.v053.i04

Semlitsch, R. D., Peterman, W. E., Anderson, T. L., Drake, D. L., & Ousterhout, B. H. (2015). Intermediate pond sizes contain the highest density, richness, and diversity of pond-breeding amphibians. *PLoS ONE*, *10*(4), e0123055. https://doi.org/10.1371/journal.pone.0123055

Shirk, A. J., Schroeder, M. A., Robb, L. A., & Cushman, S. A. (2015). Empirical validation of landscape resistance models: Insights from the Greater Sage-Grouse (*Centrocercus urophasianus*). *Landscape Ecology*, *30*(10), 1837–1850. https://doi.org/10.1007/s10980-015-0214-4

Shirk, A. J., Wallin, D. O., Cushman, S. A., Rice, C. G., & Warheit, K. I. (2010). Inferring landscape effects on gene flow: A new model selection framework. *Molecular Ecology*, *19*(17), 3603–3619. https://doi.org/10.1111/j.1365-294X.2010.04745.x

Spear, S. F., & Storfer, A. (2008). Landscape genetic structure of coastal tailed frogs (*Ascaphus truei*) in protected vs. managed forests. *Molecular Ecology*, *17*(21), 4642–4656. https://doi.org/10.1111/j.1365-294X.2008.03952.x

Steele, C. A., Baumsteiger, J., & Storfer, A. (2009). Influence of life-history variation on the genetic structure of two sympatric salamander taxa. *Molecular Ecology*, *18*(8), 1629–1639. https://doi.org/10.1111/j.1365-294X.2009.04135.x

Timm, B. C., McGarigal, K., Cushman, S. A., & Ganey, J. L. (2016). Multi-scale Mexican spotted owl (*Strix occidentalis lucida*) nest/roost habitat selection in Arizona and a comparison with single-scale modeling results. *Landscape Ecology*, *31*(6), 1209–1225. https://doi.org/10.1007/s10980-016-0371-0

Velo-Antón, G., Parra, J. L., Parra-Olea, G., & Zamudio, K. R. (2013). Tracking climate change in a dispersal-limited species: Reduced spatial and genetic connectivity in a montane salamander. *Molecular Ecology*, *22*(12), 3261–3278. https://doi.org/10.1111/mec.12310

Veysey, J. S., Babbitt, K. J., & Cooper, A. (2009). An experimental assessment of buffer width: Implications for salamander migratory behavior. *Biological Conservation*, *142*(10), 2227–2239. https://doi.org/10.1016/j.biocon.2009.04.024

Waples, R. S., & Anderson, E. C. (2017). Purging putative siblings from population genetic data sets: A cautionary view. *Molecular Ecology*, *26*(5), 1211–1224. https://doi.org/10.1111/mec.14022

Wasserman, T. N., Cushman, S. A., Schwartz, M. K., & Wallin, D. O. (2010). Spatial scaling and multi-model inference in landscape genetics: *Martes americana* in northern Idaho. *Landscape Ecology*, *25*(10), 1601–1612. https://doi.org/10.1007/s10980-010-9525-7

Watts, A. G., Schlichting, P. E., Billerman, S. M., Jesmer, B. R., Micheletti, S., Fortin, M.-J., … Murphy, M. A. (2015). How spatio-temporal habitat connectivity affects amphibian genetic structure. *Frontiers in Genetics*, *6*. https://doi.org/10.3389/fgene.2015.00275

Whiteley, A. R., Fitzpatrick, S. W., Funk, W. C., & Tallmon, D. A. (2015). Genetic rescue to the rescue. *Trends in Ecology & Evolution*, *30*(1), 42–49. https://doi.org/10.1016/j.tree.2014.10.009

Whiteley, A. R., McGarigal, K., & Schwartz, M. K. (2014). Pronounced differences in genetic structure despite overall ecological similarity for two Ambystoma salamanders in the same landscape. *Conservation Genetics*, *15*(3), 573–591. https://doi.org/10.1007/s10592-014-0562-7

Wiens, J. A. (1989). Spatial scaling in ecology. *Functional Ecology*, *3*(4), 385. https://doi.org/10.2307/2389612

Zeller, K. A., Jennings, M. K., Vickers, T. W., Ernest, H. B., Cushman, S. A., & Boyce, W. M. (2018). Are all data types and connectivity models created equal? Validating common connectivity approaches with dispersal data. *Diversity and Distributions*, *24*(7), 868–879. https://doi.org/10.1111/ddi.12742

Zeller, K. A., McGarigal, K., Beier, P., Cushman, S. A., Vickers, T. W., & Boyce, W. M. (2014). Sensitivity of landscape resistance estimates based on point selection functions to scale and behavioral state: Pumas as a case study. *Landscape Ecology*, *29*(3), 541–557. https://doi.org/10.1007/s10980-014-9991-4

Zeller, K. A., Vickers, T. W., Ernest, H. B., & Boyce, W. M. (2017). Multi-level, multi-scale resource selection functions and resistance surfaces for conservation planning: Pumas as a case study. *PLoS ONE*, *12*(6), e0179570. https://doi.org/10.1371/journal.pone.0179570

Zellmer, A. J., & Knowles, L. L. (2009). Disentangling the effects of historic vs. contemporary landscape structure on population genetic divergence. *Molecular Ecology*, *18*(17), 3593–3602. https://doi.org/10.1111/j.1365-294X.2009.04305.x

SUPPORTING INFORMATION

Additional supporting information may be found online in the Supporting Information section at the end of the article.

How to cite this article: Winiarski KJ, Peterman WE, Whiteley AR, McGarigal K. Multiscale resistant kernel surfaces derived from inferred gene flow: An application with vernal pool breeding salamanders. *Mol Ecol Resour*. 2019;00:1–17. https://doi.org/10.1111/1755-0998.13089